JOURNAL OF GUIDANCE, CONTROL, AND DYNAMICS
Vol. 28, No. 6, November–December 2005

Star Pattern Identification Using Discrete Attitude Variation Technique

G. Nagendra Rao*
Indian Space Research Organization, Bangalore 560 058, India
M. Seetharama Bhat†
Indian Institute of Science, Bangalore 560 012, India
and
T. K. Alex‡
Indian Space Research Organization, Bangalore 560 058, India

Two star pattern identification methods that use a discrete attitude variation algorithm are presented. When a spacecraft is lost in space, these methods determine the inertial attitude of the platform iteratively, starting with a hypothesis corresponding to a pair of the brightest measured and reference stars. In the first method, the spurious match of the pairs is avoided by using the magnitude of the stars in conjunction with an angular separation database. In the second, a novel spiral search on an index to the catalog star magnitude replaces the separation database. Attitude is confirmed with the identification of the remaining star vectors transformed from the spacecraft body to the inertial reference frame with the discrete attitude. These procedures are subject to numerical simulation tests along with another contemporary star identification algorithm. The new methods result in a successful star identification rate close to 100% with a process time average of a few milliseconds for reasonable perturbation of measurements. The first method shows an overall improvement compared to the reference algorithm, whereas the second one is faster only at the lower brightness noise of the star tracker.

Introduction

STARS, the true direction indicators in the sky, are denoted by their brightness and a fixed orientation with respect to each other. Easily identifiable patterns of bright stars called constellations have been recorded by humans since time immemorial. Even modern day spacecraft, fitted with star trackers,[1] observe the stars routinely to determine the attitude of the platform and update the gyroscopes for attitude control. However, each observation is matched with the proper reference catalog star before the determination of the spacecraft attitude. The star identification is carried out, initially, when the spacecraft is hurled into outer space after the launch and, subsequently, when its attitude is known and stabilized (normal phase). The first phase is called lost-in-space (LIS) because the orientation of the spacecraft represented by the inertial-to-body $\boldsymbol{D}_{I \to B}$ direction cosine matrix (DCM) is generally not known.

The problem of automatic star pattern identification for real-time spacecraft attitude determination is widely investigated. Gottlieb and Wertz[2] classified the various star identification algorithms into direct match, angular separation or polygon match, phase match, and discrete attitude variation techniques. Van Bezooijen[3] provided a clever enhancement to the polygon match method by using a sorted array of bright stars whose precomputed angular separation is confined to the field of view (FOV) of the star tracker. Baldini et al.[4] extended the polygon match technique to a narrow FOV star tracker. They observed that the time required to identify a star constellation depends primarily on the two brightest stars because only a few low-magnitude stars are present in the reference catalog. The presence of bright stars in the measured set increases the information content and reduces the possibility of mismatches with other faint stars in the catalog.[4] A recent algorithm by Padgett and Delgado[5] established a correlation of the star pattern over a grid centered on a pivotal star with that of the stored pattern in a database.

Discrete Attitude Variation Method

In the discrete attitude variation (DAV) method, a hypothesis is made about the inertial attitude of the spacecraft. The observed star pattern is transformed from the body to the inertial reference frame or vice versa with the assumed attitude, and the hypothesis is verified by the presence of matching stars in the onboard reference catalog. If the hypothesis is correct, the assumed attitude is returned. Otherwise another discrete attitude is attempted till all of the possible options are exhausted. If an initial attitude estimate of the spacecraft is known a priori, the iteration can conveniently be started from that orientation. The advantage of this method is that the attitude of the spacecraft is directly available after a successful star pattern identification, instead of mere catalog numbers of the matched stars as given by the other methods. However, no simple technique is available, without the excessive search involved, to confirm the presence or absence of a star in the catalog. In addition, the iterative nature of the algorithm involves a large amount of computation. Gottlieb and Wertz[2] recommend the DAV method to be used only as a last resort, if all other identification methods fail.

Survey of Previous Work

Blanton[6] experimented with the DAV technique and used the well-known triad method[7] that forms an orthonormal basis to transform the vectors from the reference catalog to the image plane of the observation sensor. Markley[8] gave a detailed analysis of the attitude determination for the two-vectors observation case that includes the triad method. The triad method is a quick-and-dirty estimator of the attitude because it uses only two vector observations. Even then, the size of the computational load prohibits the application of Blanton's method for onboard star identification.

Bank[9] described a star tracker that identifies stars from LIS condition using a DAV algorithm in conjunction with a separation

Received 9 July 2004; revision received 4 March 2005; accepted for publication 21 April 2005.

*Head, Star Sensors and Computer Systems Division, Laboratory for Electro-Optics Systems, 1st Cross, 1st Stage, Peenya Industrial Estate; gnrao@leosisro.com. Member AIAA.

†Professor, Aerospace Engineering Department; msbdc1@aero.iisc.ernet.in.

‡Director, Laboratory for Electro-Optics Systems, 1st Cross, 1st Stage, Peenya Industrial Estate; tkalex@vsnl.com.

database. The identification method he outlined does not make use of the magnitude of the stars but only depends on the angular separation between the measured star pairs. He reported long solution times for LIS cases, which range from 1 to 200 s.

Star trackers[10,11] are used for fine pointing of the SPOT5 satellite and the International Space Station. The pattern recognition algorithm[3] employed in the described star trackers begins to identify the stars with a pre-computed and sorted angular separation database of guide stars. After the match of the candidate stars is obtained, a check is usually made to ascertain the difference between their measured and reference magnitudes to lie within a specified tolerance.

Mortari et al.[12] identified the star pattern in LIS condition starting with a pair of measured stars. A list of probable star pairs is drawn from an ordered database (K vector) (see Ref. 13) using the angular separation between the measured stars as index. Similarly, probable star pairs are drawn based on all of the sides and diagonals of a four-star polygon called a pyramid. A consistency check made on the selected star pairs yields a unique match with the reference catalog. This reference pyramid is then used to identify the remaining stars in the constellation. This popular procedure relies only on the angular separation of the stars, but does not take their magnitude into account.

Scope of the Paper

In this paper, we propose two new methods, hashing algorithms for star pattern identification, HASPID-K and HASPID-M, for LIS condition using the DAV technique that consider the star magnitudes in addition to their separation. In addition to the LIS condition, the proposed algorithms have a provision to use a priori estimate of the initial attitude. These methods are an improvement over existing DAV techniques.[2,6,9] We sharpen and apply a software tool spiral search,[14] originally developed for robotics research, to match the brightness and angular separation of the observed star pair to that of the catalog. We demonstrate the use of our newly developed fast star-detection technique.[15] The HASPID-M method is inherently not limited by the FOV of the star tracker, unlike the earlier methods and, hence, is more suitable to the observations of the extended FOV[16] or multiple star trackers.

In the following sections, the algorithms are described in detail. The new algorithms are coded and subjected to numerical simulation tests[17] along with a reference algorithm Pyramid.[12] The results are compared to bring out the advantages and the limitations of the proposed new techniques.

Algorithm

We present the key ideas first. Because we intend to use the star magnitude in our algorithms, we briefly mention the limitations and the advantages of this approach in the following subsection. The procedure to form an index to the magnitude field in the star catalog is described next. The next subsection deals with grading the measurements of the star tracker. The next one specifies the underlying assumptions about the identification problem. The following subsections present the details of the algorithms.

Star Magnitude

Although a star tracker can measure the location of a star in its FOV to a subarcsecond precision using a hyperacuity technique,[1] its brightness measurement capability has certain limitations. The apparent brightness of a star as detected by the tracker is denoted as instrument magnitude (IM), which differs from the brightness level perceived by the human eye, cataloged as visual magnitude (VM). The IM of a star may vary with the spectral response and the dark current of the detector of the star tracker, the background illumination, the detection method, the star position in the FOV, and the angular rate of the platform, and in addition may not even be stable with time. Hence, many researchers[5,13] feel that the magnitude should not be used for star identification. A contrasting view is that the star magnitude is an independent feature in the pattern recognition that will enhance the pattern dimension and, hence, the uniqueness of the star constellation within the star catalog.[3,4,11] We support this view for the following reasons.

Let us assume that an onboard star catalog with N entries is selected[15] from the sky with a uniform star density. A star tracker simultaneously observes n celestial objects within its FOV (Φ), with an angular measurement precision σ_p. We consider two objects at a time, for example, i and j ($i, j \in [1, \ldots, n]$), with unit vectors $\boldsymbol{W}_i$ and $\boldsymbol{W}_j$, respectively, with a separation angle ϑ_{ij} between them, that is, $\cos(\vartheta_{ij}) = \boldsymbol{W}_i^T \boldsymbol{W}_j$. Then the expected frequency f_{ij} of matches that may occur randomly between the measured objects and the combination of stars in the catalog is given as[12]

$$f_{ij} = [N(N-1)/2]\sin(\delta)\sin(\vartheta_{ij}), \qquad 0 < \delta < \vartheta_{ij} \le \Phi \quad (1)$$

Equation (1) can be viewed as the product of two terms,

$$f_{ij} = {}^{N}C_2 \cdot \mathcal{P}(\theta = \vartheta_{ij}) \quad (2)$$

where

$${}^{N}C_2 \triangleq N(N-1)/2 \quad (3)$$

$$\mathcal{P}(\theta = \vartheta_{ij}) \triangleq \sin(\delta)\sin(\vartheta_{ij}) \quad (4)$$

The term ${}^{N}C_2$ in Eq. (3) refers to the total number of combinations that can be drawn from N catalog stars with two at a time. The term $\mathcal{P}(\theta = \vartheta_{ij})$ in Eq. (4) gives the probability that the separation angle θ of any of the drawn pair (denoted by $a, b \in [1, \ldots, N]$ and $a \neq b$) satisfies the condition $[(\vartheta_{ij} - \delta) \le \theta_{ab} \le (\vartheta_{ij} + \delta)]$. The error term δ in the Eqs. (1) and (4) denotes the uncertainty in the angle measurement and is generally denoted as $k\sigma_p$, where $k \in [1, 2, 3]$ depending on the confidence level. However, k is set to 6.4 based on experimentation to suit the observed star density and the selected FOV of the star tracker in Ref. 12.

If the star tracker has an additional ability to measure the brightness of those celestial objects, for example m_i and m_j magnitudes, respectively, with a precision of σ_m, then it can be made use of to reduce the spurious matches. Equation (2) can be modified by imposing an additional condition that matches the star magnitudes as follows:

$$f_{ij} = {}^{N}C_2 \cdot \mathcal{P}(\theta = \vartheta_{ij}) \cdot \mathcal{P}(m_{a,b} = m_{i,j}) \quad (5)$$

where

$$\mathcal{P}(m_{a,b} = m_{i,j}) = \mathcal{P}(m_a = m_i) \cdot \mathcal{P}(m_b = m_j) + \mathcal{P}(m_a = m_j) \cdot \mathcal{P}(m_b = m_i) \quad (6)$$

$$\mathcal{P}(m_a = m_i) \triangleq \mathcal{P}(m_i - 3\sigma_m \le m_a \le m_i + 3\sigma_m) \quad (7)$$

$$\mathcal{P}(m_a = m_j) \triangleq \mathcal{P}(m_j - 3\sigma_m \le m_a \le m_j + 3\sigma_m) \quad (8)$$

$$\mathcal{P}(m_b = m_i) \triangleq \mathcal{P}(m_i - 3\sigma_m \le m_b \le m_i + 3\sigma_m) \quad (9)$$

$$\mathcal{P}(m_b = m_j) \triangleq \mathcal{P}(m_j - 3\sigma_m \le m_b \le m_j + 3\sigma_m) \quad (10)$$

Here, the terms $\mathcal{P}(m_a = m_i)$ and $\mathcal{P}(m_b = m_j)$, etc., in Eqs. (7–10) refer to the probability of occurrence of the stars (a and b) in the pair drawn randomly from the catalog that match the magnitude of the measured objects (i and j) within the precision of the tracker. If the distribution of the stars in the onboard catalog is known, the probability measures $\mathcal{P}(m_a = m_i)$, etc., can be evaluated.

An example probability density function (PDF) and a cumulative distribution function (CDF) of the star catalog C used in this study (with $N = 1613$ entries) are given in the Table 1. These are obtained by binning the stars in the catalog with 0.5 magnitude interval. The first column x in Table 1 gives the IM of the stars at the end of each bin, the second column, denoted by $p(x)$, gives the PDF, and the third column, denoted by $F(x)$, gives the CDF of each bin, respectively. Refer to Figs. 1a and 1b for the $p(x)$ and $F(x)$ curves. The occurrence probability $\mathcal{P}(m = m_i)$ of a star with m_i magnitude brightness can be computed by calculating the area under the $p(x)$

Table 1 Probability distribution of stars in onboard catalog *C*

x[a]	$p(x)$	$F(x)$
0.0	0.0025	0.0025
0.5	0.0025	0.0050
1.0	0.0025	0.0074
1.5	0.0062	0.0136
2.0	0.0155	0.0291
2.5	0.0254	0.0546
3.0	0.0465	0.1011
3.5	0.0756	0.1767
4.0	0.1358	0.3125
4.5	0.2443	0.5567
5.0	0.4433	1.0000

[a]Here x is IM of stars at upper limit of each bin.

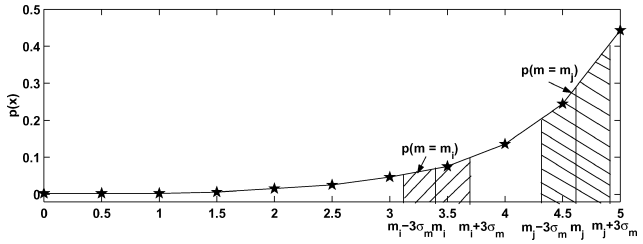

a) Probability density function of stars in catalog *C*

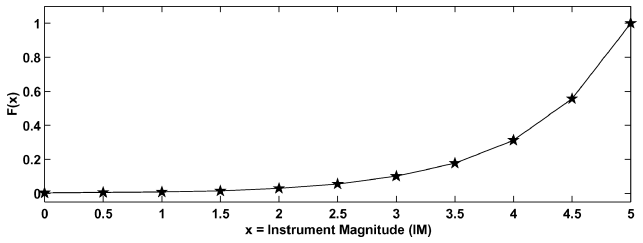

b) Cumulative distribution function of stars in catalog *C*

Fig. 1 Star distribution in onboard catalog.

curve that spans from $(m_i - 3\sigma_m)$ to $(m_i + 3\sigma_m)$ in the x axis as follows:

$$\mathcal{P}(m = m_i) = \int_{m_i - 3\sigma_m}^{m_i + 3\sigma_m} p(x)\,\mathrm{d}x \tag{11}$$

$$\mathcal{P}(m = m_i) = F(m_i + 3\sigma_m) - F(m_i - 3\sigma_m) \tag{12}$$

The value of $\mathcal{P}(m = m_i)$ in Eq. (12) can either be inferred from the graph in Fig. 1b or calculated by interpolation of third column in Table 1. Equations (5) and (6) can be simplified as

$$f_{ij} = 2 \cdot {}^{N}C_2 \cdot \mathcal{P}(\theta = \vartheta_{ij}) \cdot \mathcal{P}(m = m_i) \cdot \mathcal{P}(m = m_j) \tag{13}$$

because

$$\mathcal{P}(m_{a,b} = m_{i,j}) = 2\mathcal{P}(m = m_i) \cdot \mathcal{P}(m = m_j) \tag{14}$$

Let us consolidate the theory with an example of $N = 1613$, $m_i = 3.4$, $m_j = 4.6$, $\vartheta_{ij} = 8.382$ deg, $\sigma_m = 0.3$ magnitude, and $\sigma_p = 32.7$ arc-s. The expected frequency of random matches f_{ij} is 192 per Eq. (1), but reduces to 120 (63%) spurious matches when star magnitudes are considered as per Eq. (13). Had another pair of stars with magnitudes $m_i = 1.9$ and $m_j = 3.2$ been observed, but with the same parameters as in preceding example, then the expectation of random matches falls to only 9 (5%). This is due to the low probability of occurrence of a bright star (small area a star of a lower magnitude occupies under the PDF curve), when compared to a faint star. Compare the areas pertaining to the stars of m_i and m_j $(m_i < m_j)$ in Fig. 1a. Hence, it is advantageous to select stars in their ascending order of magnitude from any given set of n measurements to reduce spurious matches with the catalog. An integer array of n rows, called as the index to the star magnitude measurement (StarIndex), can be formed to facilitate the selection. The first row in this index points to the brightest star measured, the second to the second brightest and so on.

The probability models in Eqs. (1) and (13) are verified by Monte Carlo simulations and are found to be accurate subject to the actual distribution of stars in the sky. However, the number of random matches with the catalog that occur with only a pair of measurements is clearly not acceptable, whether the magnitude of the stars is considered or not. Polygon match star identification algorithms[3,12,13] use additional information, such as the angular separation of a few more sides or diagonals of the star polygon (${}^{n}C_2$, where $n \geq 4$ vertices), to reduce the occurrence of spurious matches to a level of 10^{-7} or below. We propose two alternative approaches (HASPID-K and HASPID-M methods) using the DAV technique that are described later. The magnitude information helps to reduce the range of candidate stars suitable to form the pivotal stars in both these methods. This speeds up the identification and eliminates false matches.

Correct star identification is of great importance in a LIS situation when no help from other attitude sensors is forthcoming. It is vital to combine and utilize all of the information available for the survival of the spacecraft. Hence, we decide to use the star magnitude information in these procedures. Note, however, that this scheme depends on the capability of the available star tracker hardware.[9,10,18]

Index to Magnitude

The concept of index to the magnitude mentioned earlier can even be extended to the reference star catalog. A sorted array, magnitude index (MI) may be formed with the star catalog indexes such that magnitude $[\mathrm{MI}(i)] \leq$ magnitude $[\mathrm{MI}(i+1)]$, $i = 1, \ldots, N$, where magnitude $[k]$ is the magnitude of the kth star. A function $k_{\mathrm{MI}}(m)$ can be determined such that it returns the index k of the array MI, given the star magnitude m. The relation of the MI with the magnitude of stars in catalog C is shown in Fig. 2. An empirical function that approximates the preceding relation with error limits $[-29, 22]$ is

$$k_{\mathrm{MI}}(m) = \exp(1.1601m + 1.5889) \tag{15}$$

Equation (15) helps to compute the range of stars required in the search procedures. The MI array facilitates access of the stars from the reference catalog in their order of magnitude. The utility of this MI will be described in later sections.

Measurements

The measurements made from a properly calibrated star tracker usually resemble Gaussian distribution. This is characterized by the well-known bell-shaped PDF with the peak at the mean μ_m of the samples with a spread of σ_m. If a measurement falls beyond the range of $[\mu_m - 3\sigma_m, \ldots, \mu_m + 3\sigma_m]$, then we can reject it with

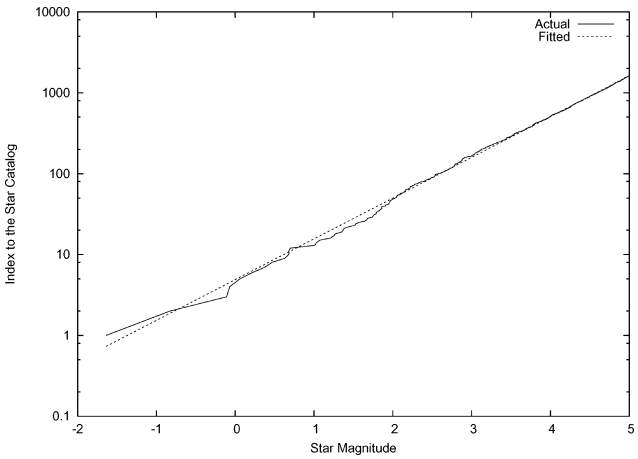

Fig. 2 Relation of magnitude to MI of catalog.

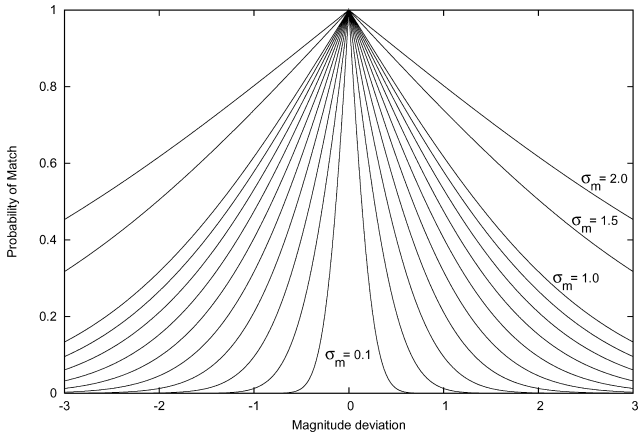

Fig. 3 Probability of star match with magnitude deviation.

99.99% confidence that the sample does not belong to the cluster characterized by $\mathcal{N}[\mu_m, \sigma_m]$. Otherwise it is accepted. Instead of this binary (accept or reject) decision, it is possible to grade each measurement whether it belongs to a known cluster. We call this attribute as the probability of the match in a scale of 0–1. If the probability is 1, then it is a perfect match, and if it is zero, then it is a poor match. One such grading function $\wp(m, \mu_m, \sigma_m)$ for any measurement m is defined as

$$z(m, \mu_m, \sigma_m) = \frac{|m - \mu_m|}{2\sigma_m} \tag{16}$$

$$\wp(m, \mu_m, \sigma_m) = 2[1 - \Phi\{z(m, \mu_m, \sigma_m)\}] \tag{17}$$

$$\Phi\{z\} = \frac{1}{\sqrt{2\pi}} \int_{-\infty}^{z} \exp(-u^2/2)\, \mathrm{d}u \tag{18}$$

where $\Phi\{z\}$ refers to the area under the unit normal curve for the random variable z and $\Phi\{0\} = 0.5$ (Ref. 19). As expected, the probability $\wp(m)$ of a star match decreases with the deviation of the measured magnitude m from its mean μ_m for different σ_m as shown in Fig. 3.

If we consider two star measurements i and j (with m_i and m_j magnitudes, respectively) at a time, then the probability $\wp(m_{ij} = m_{ab})$ of the match of this pair with that of the catalog stars a and b can be computed as follows:

$$\wp(m_{ij} = m_{ab}) = \wp(m_i, m_a, \sigma_m)\wp(m_j, m_b, \sigma_m) \tag{19}$$

Here, the terms m_a and m_b are magnitudes of stars a and b. If this probability exceeds a threshold p_{th} then we can accept that the measured pair $[i, j]$ belongs to the catalog star pair $[a, b]$, otherwise we can reject it. Equation (6) gives the probability of occurrence of a pair, whereas Eq. (19) gives the probability of match with a given catalog pair. Note that these represent different quantities, despite the similarity in notation.

Assumptions

The following assumptions are made about the star identification problem:

1) A star observed at pixel h and line v of the charge-coupled device (CCD) detector of the star tracker may be converted to a unit vector $[x_s \;\; y_s \;\; z_s]^T$ in the sensor reference frame by a function $\boldsymbol{f}_s(h, v)$ as

$$y = \frac{-(h - h_0)s_p}{f} \tag{20}$$

$$z = \frac{-(v - v_0)s_p}{f} \tag{21}$$

$$\boldsymbol{f}_s(h, v) \triangleq \begin{bmatrix} x_s \\ y_s \\ z_s \end{bmatrix} = \frac{1}{\sqrt{1 + y^2 + z^2}} \begin{bmatrix} 1 \\ y \\ z \end{bmatrix} \tag{22}$$

where s_p is the size of a pixel in millimeters, f is the effective focal length (EFL) of the optics in millimeters, and $[h_0, v_0]$ refers to the null pixel and line (typically [512, 512] for a 1024×1024 size) of the CCD at the origin of the star tracker reference frame.

2) The distance d between two stars i and j with unit vectors $\boldsymbol{W}_i$ and $\boldsymbol{W}_j$ is given in Eq. (23). It is related to the angular separation ϑ_{ij} of the vectors as follows:

$$d(\boldsymbol{W}_i, \boldsymbol{W}_j) = \|\boldsymbol{W}_i - \boldsymbol{W}_j\| = 2\sin(\vartheta_{ij}/2) \tag{23}$$

3) The tolerance of the maximum angular deviation of a star vector measurement is ϵ. It is three times the standard deviation σ_p of angular measurement precision of the star tracker by Eq. (24). If location noise σ_{pix} of the tracker is given in pixels, then σ_p expressed in radians can be computed as shown in Eq. (25). The threshold t_{angl} for the maximum deviation of the separation angle between a pair of the measured and catalog stars is given in Eq. (26). The maximum uncertainty radius t_{cone} of a cone in the projected direction of a star is shown in Eq. (27) (Ref. 15). Thus,

$$\epsilon = 3\sigma_p \tag{24}$$

where

$$\sigma_p = \sigma_{\text{pix}} s_p / f \tag{25}$$

$$t_{\text{angl}} = 4\epsilon \tag{26}$$

$$t_{\text{cone}} = 2\sin(\epsilon/2) \tag{27}$$

4) The brightness of the stars measured by the tracker corresponds to that of the respective catalog stars with a zero mean difference and a standard deviation of σ_m magnitude.

5) The star tracker is fully calibrated, and its noise characteristics σ_p and σ_m are well known before the flight.

DAV Algorithm

The objectives of the star identification problem are as follows. We have to match n celestial objects from the observations of a star tracker in LIS condition and identify the corresponding stars of an onboard catalog of N entries. At least two stars are to be identified correctly and no wrong identification is permitted. A coarse attitude matrix $\boldsymbol{D}_{I \to B}$ that can transform the stars from the inertial reference frame to the tracker frame is to be given as output. The algorithm may accept an a priori estimate of the attitude of the platform to speedup the identification.

We convert the LIS problem to a set of probable discretely known attitudes. These probable attitudes are then rated for the presence of the catalog stars that match the observations. The initial hypothesis is formed with the sights of two bright stars used in conjunction with either an angular separation database (K vector) of the catalog or an index to the catalog star magnitudes (MI) array. As a result, two variations of our DAV algorithm are born. We shall present an overview of both the methods first and describe the logic flow of the algorithms later.

HASPID-K Method

In the first method, HASPID-K, two bright stars i and j ($i, j \in [1, \ldots, n]$) are selected as guide stars using the StarIndex array. These are processed further only if they are farther than t_{near}, that is, only if $d(\boldsymbol{W}_i, \boldsymbol{W}_j)^2 > t_{\text{near}}$ to avoid coaligned vectors. With the help of their separation angle ϑ_{ij} as index and its measurement tolerance $\pm 2\epsilon$, a list of probable star pairs is drawn from the K-vector database.[13] The probability of match of the measured magnitudes of star pair $\wp(m_{ij} = m_{ab})$ with that of each probable reference pair $[a, b]$ ($a, b \in [1, \ldots, N]$) is computed. The pairs with a probability $\wp(m_{ij} = m_{ab}) < p_{\text{th}}$ are filtered out as spurious star matches.

With an assumption that each of the remaining r catalog star pairs match the observed pivotal stars, a set of discrete inertial attitudes are formed by direction cosine matrices $\boldsymbol{D}_i, i = 1, \ldots, r$, with the Triad method. These matrices are used sequentially to project the remaining star observations into the reference frame $\boldsymbol{V}_j$ as given by Eq. (28). Instead of converting all of the stars in the catalog to the image plane,[6] we project only the remaining stars observed in

the tracker reference frame to the inertial frame with the computed attitude matrix $\boldsymbol{D}_i^T$. Because the stars measured are always fewer than those that are present in the catalog ($n < N$), the computational burden is accordingly reduced. The presence of the projected stars in the three-dimensional space of the reference frame is confirmed with the hash search technique described in Ref. 15. Any catalog star that is closest to the projected vector direction $\boldsymbol{V}_j$ within an uncertainty radius of t_{cone}, and corresponds to the observed star's magnitude, is accepted as a match.[15]

The set of discrete attitudes $\boldsymbol{D}_i$ are rated with a loss function based on the identity of the remaining stars sighted. The loss function $L(\boldsymbol{D}_i)$ given in Eq. (29) measures the degree of match of the observed star pattern with that of the catalog. Thus,

$$\boldsymbol{V}_j = \boldsymbol{D}_i^T \boldsymbol{W}_j, \qquad j = 1, \ldots, n \tag{28}$$

$$L(\boldsymbol{D}_i) = \sum_{j=1}^{n} a_j \|\boldsymbol{U}_j - \boldsymbol{V}_j\|^2, \qquad i = 1, \ldots, r \tag{29}$$

where $\boldsymbol{U}_j$ and $\boldsymbol{W}_j$ are the vectors of the jth star in inertial frame and the tracker frame, respectively, and a_j is the weight of each measurement. The attitude matrix that identifies the most stars with the minimum loss is returned as the final output matrix $\hat{\boldsymbol{D}}_{I \to B}$.

HASPID-M Method

In the second algorithm, we rely on the brightness information provided by the star tracker and restrict the selection range of guide stars by the magnitude of the stars measured. The initial hypothesis is formed by a spiral search[14] carried on MI to the star catalog. In such cases, the LIS star identification can be achieved without the support of the angular separation database (K vector). This is particularly suitable for fast embedded processors with little onboard memory. This method is HASPID-M.

A crucial step in the HASPID-M method is to arrive at the initial hypothesis about the attitude. At least two stars of the measurement and reference stars are required to be matched to form an attitude matrix. If two stars are taken out of N catalog stars at a time, it needs ${}^N C_2$ computations of the angular separations. For example, if $N = 1613$, this amounts to 1,300,078 computations. This is a large search space. The index to catalog star magnitude (MI) described earlier can be used to reduce the search effort. Because σ_m is the precision of the measurement of brightness, the observed star of m magnitude can only be one of the catalog stars in the range of $[\text{MI}(k_{\min}), \ldots, \text{MI}(k_{\max})]$, where $k_{\min} = \max[1, k_{\text{MI}}(m - 3\sigma_m)]$ and $k_{\max} = \min[(k_{\text{MI}}(m + 3\sigma_m), N]$.

Two bright stars, for example, p and q, are to be matched. These stars are selected in ascending order of their magnitudes using the StarIndex array due to reasons mentioned earlier. The search space then confines to a rectangular grid that is bounded by $[\text{MI}(p_{\min}), \ldots, \text{MI}(p_{\max})]$ on one side and $[\text{MI}(q_{\min}), \ldots, \text{MI}(q_{\max})]$ on the other side, where $p_{\min}$, $p_{\max}$, $q_{\min}$, and $q_{\max}$ refer to the bounds of MI for the pth and qth star, respectively.

Continuing with the example, if $m_p = 1.9$, $m_q = 3.2$, and $\sigma_m = 0.3$, then $[\text{MI}(16), \ldots, \text{MI}(126)]$ and $[\text{MI}(71), \ldots, \text{MI}(570)]$ are the bounds. Total search space reduces to 55,500 (111×500, both ends included) points, that is, only 4.5% of the original combinations. A smaller example search space is shown in Fig. 4 for clarity. The task is to locate a point (p_n, q_n) on this grid that indicate the stars $[a, b]$ of the catalog [where $a = \text{MI}(p_n)$, $b = \text{MI}(q_n)$] and verify whether that catalog pair's angular separation matches that of the pair measured. A catalog pair is identified as a guide star pair, only if the following condition is true:

$$|\vartheta_{ab} - \vartheta_{pq}| < t_{\text{angl}} \tag{30}$$

where ϑ_{ab} is the separation angle between the unit vectors $\boldsymbol{U}_a$ and $\boldsymbol{U}_b$ of the selected catalog star pair $[a, b]$ and ϑ_{pq} is the separation angle between the unit vectors $\boldsymbol{W}_p$ and $\boldsymbol{W}_q$ of the star pair $[p, q]$ considered.

One simple search strategy is to carry out a raster scan, that is, row by row starting from the top, to explore every point in this search space. Because the brightness noise is Gaussian in nature, the reference star pair is most likely to be found close to the center of the search space given by $(p_{\text{mid}}, q_{\text{mid}})$, where $p_{\text{mid}} = k_{\text{MI}}(m_p)$ and $q_{\text{mid}} = k_{\text{MI}}(m_q)$. In view of this, a spiral search[14] that starts from $(p_{\text{mid}}, q_{\text{mid}})$ and expands radially can reduce the search time significantly. The spiral search algorithm is explained next. Note that Bayesian criteria to choose the reference star pair with the best possible magnitude match are met by the selection of a candidate star pair that is closest to the center $[p_{\text{mid}}, q_{\text{mid}}]$ of the search space. Thus, the travel path chosen by the spiral search automatically minimizes the probability of false star identification.

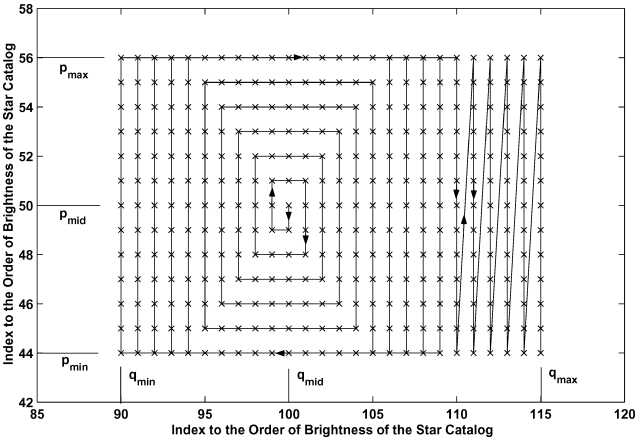

Fig. 4 Search space exploration using spiral grid.

The discrete attitude matrices are formed by the pairs of identified guide stars and the measured stars with the Triad method. These matrices are rated for the match of the other star observations as described earlier.

Spiral Search

Our spiral search algorithm closely follows the method of Hall,[14] but returns one grid point at a time instead of the entire spiral path at once. It is essentially a "bed bug" algorithm that starts a bug at the center with a soft limit on each side (north, south, east, and west) set to ± 1 of the center initially. The coordinates of the bug are returned as the bug hops one step each on the grid. If the bug touches any of the soft limits, it is deflected to the adjoining side, and the corresponding limit is increased by 1 unless it is a bound (hard limit) of the search space. Each grid point is visited only once, and the bug can hop to next possible step in that direction. If the bug covers the entire space, then the search is terminated. A typical path traced by a bug in a spiral search is shown by the arrows in Fig. 4.

Logic Flow

The overall logic flow of the new DAV algorithm is shown in Fig. 5. The block "identify stars" is detailed in Fig. 6. The step "find probable reference star pair" (in Fig. 6) is expanded in Fig. 7. In the first step in Fig. 5, an index (StarIndex) is formed to pick the measured stars in ascending order of their magnitudes. If the initial attitude of the platform is known, each measured star vector is projected to the inertial sphere using the a priori attitude $\boldsymbol{D}_{B \to I}$. Stars that fall within a cone of radius σ_{AD} attitude uncertainty centered around each of the projected stars' directions are selected from the catalog using the hash search technique given in Ref. 15. A partial catalog is formed after eliminating the duplicate reference stars. In LIS case, the entire reference catalog is selected. The array MI described earlier is formed with the magnitude entries of the selected catalog.

In the identify stars block shown in Fig. 6, two bright stars (pivotal stars) that are separated more than t_{near} are selected using StarIndex array. A set of probable reference star pairs that matches the observation is selected in the next step. The attitude DCM is formed using the Triad method with the first reference star pair and the selected observation pair. The remaining observed stars are projected

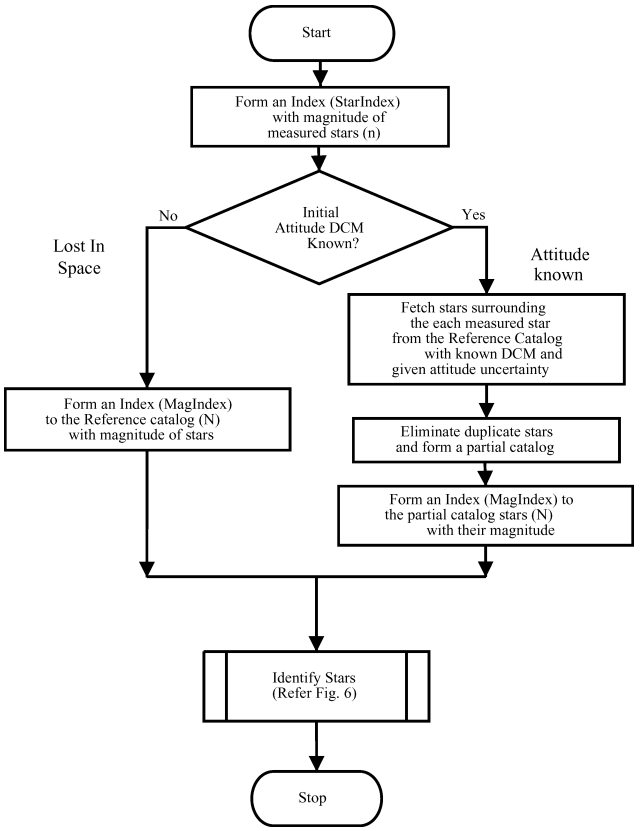

Fig. 5 Flowchart of star identification, part 1.

to inertial sphere using the computed DCM. The catalog is searched for stars that fall within t_{cone} distance of the projected star direction using the hash search procedure. The loss function given in Eq. (29) is computed with the measured and corresponding identified stars. The star pattern identified with the minimum loss is stored. The procedure is iterated until either at least four or more stars are identified or until all of the combinations of the reference pairs and measured stars are exhausted. Double stars are eliminated from the list of the identified due to their ambiguity. If at least two stars remain in the list of the identified, then the program returns success, otherwise it returns silence.

In the find probable reference star pair block shown in Fig. 7, the program branches to HASPID-K or HASPID-M routines, depending on whether an angular separation database is to be used or not. In the HASPID-K procedure, the reference star pairs that match the measured star pair separation are fetched using the K-vector database. The probability of match between the magnitudes of the selected catalog pairs with that of the measured pair is computed as per Eq. (19). Pairs with match probability that fall below the set threshold p_{th} are filtered out. In the HASPID-M method case, the reference pairs that match the measured stars better than t_{angl} are selected using the spiral search routine carried out on MI array. These probable reference star pairs are returned sequentially.

This completes the description of the star identification algorithm using the DAV technique. In the next section, we present the evaluation of the new algorithm under various stress conditions.

Numerical Simulation

To evaluate the proposed new star identification methods, Monte Carlo numerical simulations are conducted. Earlier, Padgett et al.[17] carried out a systematic study of three representative star pattern identification algorithms, namely, triangle, match group, and grid algorithms. They established a standard test suite for comparing the percentage of successful star identifications with these algorithms. To determine the relative performance of the new algorithms, they are subjected to the same battery of tests prescribed by Padgett et al., along with another contemporary star identification algorithm,

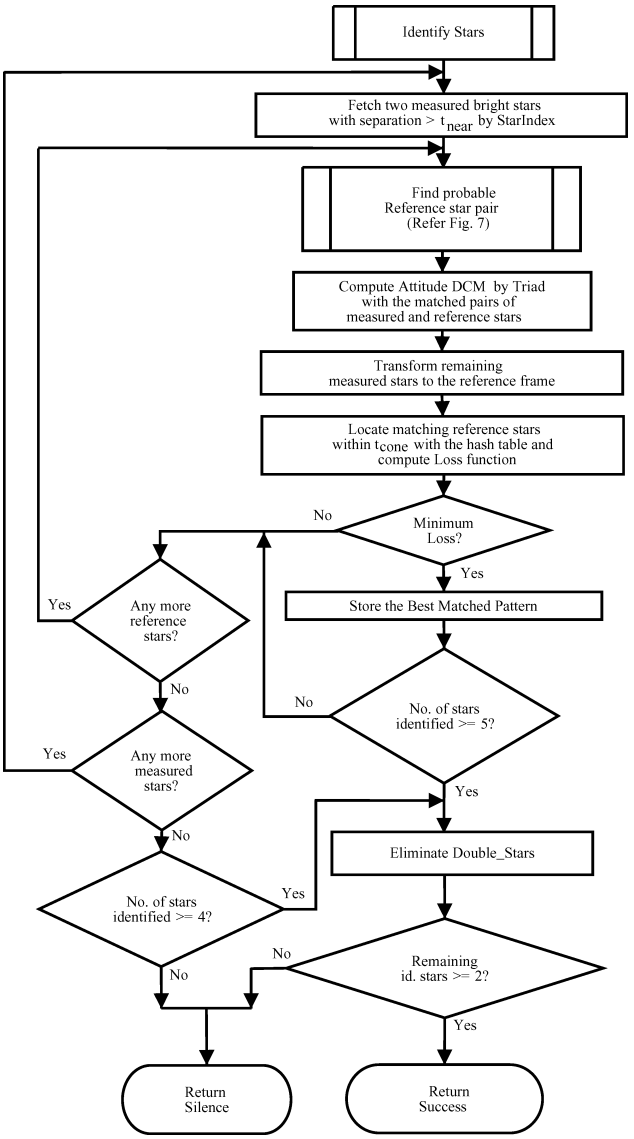

Fig. 6 Flowchart of star identification, part 2.

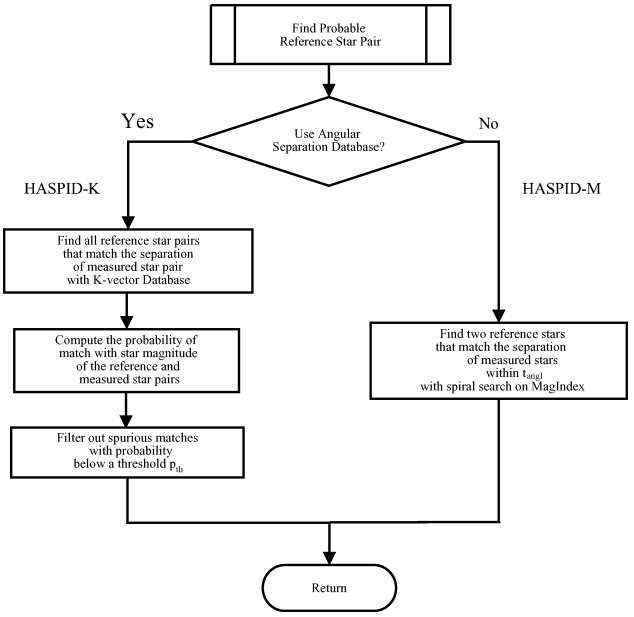

Fig. 7 Flowchart of star identification, part 3.

Pyramid, and the results are compared. We have implemented Pyramid algorithm and tested it independently as per the details available from the literature[12,13] only for academic purposes.

Notes

1) The simulated star tracker FOV is 20×20 deg, and the EFL of the optics is 44.122 mm. The CCD detector consists of 1024 rows of 1024 pixels each (14.336-mm size each side). The size of each pixel s_p is 0.014 mm.

2) The onboard star catalog C contains 1613 entries of stars, N, with a limiting magnitude of 5.0 VM extracted from the SKYMAP-2000 reference star catalog.[15] Table 1 gives the probability distribution of the stars in the selected onboard catalog. Figure 1 shows the PDF and CDF curves.

3) The data fields for each star in C consist of the three direction cosines of the stars and the IM of the star. The star positions in C are perturbed by 1 arc-s noise (1σ), and brightness values are perturbed by 0.1 stellar magnitude (1σ) from their mean values to represent the errors that occur in the catalog-generation process.[11,17] In the case of multiple stars that are closer to each other by less than 0.2-deg angular separation (limited by the resolving power of the tracker optics), only the brightest star is retained with an appropriate flag (DOUBLE_STAR) in C (Ref. 15).

4) The simulation star catalog S is another subset of SKYMAP-2000 catalog limited up to 7.5 VM. This consists of around 27,000 stars. No star is deleted from or added to this catalog.

5) The star tracker is made to orient in a random direction, and all the stars in the FOV are selected. Gaussian noise is added for both location and brightness to simulate the measurement process. For processing, 10 stars that are brighter than the limiting magnitude of the tracker (5.0 IM) in each frame are selected, that is, the number of stars, n, seen in an observation frame is 10.

6) As a result of adding noise to the brightness, a few faint stars may shine brighter than the limiting magnitude and, hence, appear in the measurements. Because these are not present in the C, such stars simulate the spikes (debris, variable stars, or other messier objects) in the measurements. Table 2 shows the statistics of the spikes simulation as a function of the brightness error and the number of frames where at least four stars of C are present in the FOV. Note that even under zero noise conditions, the entries in C do not match the observations exactly due to the imperfect catalog-generation mentioned in note 3.

7) If a frame consists of less than 10 stars, it is discarded and another frame is simulated. It provides adequate stars to identification algorithms even in the presence of spikes but excludes the effect of star availability in the celestial sphere. This assumption can easily be satisfied in LIS case by reorienting the star tracker in another direction, when there are insufficient number of stars in an observed frame.

8) Data files that contain the star measurements (location and brightness) for 1000 frames of exposure are fed as inputs to all of the star identification algorithms, HASPID-K, HASPID-M, and Pyramid, and their performances are logged for various test conditions. Note that the Pyramid method does not use the brightness of the star.

9) Tests are repeated to determine the sensitivity of star identification for each variable combination, namely, location and brightness noise for LIS case. The methodology of keeping one variable constant while varying the other as described by Padgett et al. in Ref. 17 is followed.

10) The thresholds t_{angl} and t_{cone} are changed for the HASPID method appropriately with each test case.[17] In the case of zero noise simulation, the thresholds corresponding to the tracker noise values of $\sigma_{\text{pix}} = 0.5$ pixel and $\sigma_m = 0.3$ magnitude, are used. The distance threshold t_{near} to avoid the coaligned star vectors is set to 0.001, which roughly corresponds to 1.8-deg separation angle between them. The threshold for probability of match of the pair p_{th} is set to 0.05. The allocated hash table size is assumed to be three times the catalog size, $3N$, with a table-load-factor α equal to 0.33 to speed up the catalog access.[15]

11) In the case of the Pyramid method,[12] the tolerance on the random star pattern match is set to 1. If the analytical probability exceeds this value, the attempt to match that star triad in the catalog is abandoned. The K-vector angular separation database consists of 71,834 entries for the given catalog C. The parameter ϵ that is used to fetch the admissible star pairs from the K-vector database[13] is varied per Eq. (24).

12) In a frame, at least two of the simulated stars are identified correctly, that is, categorized as successful identification. If the algorithm returns no identified stars or less than the minimum required, then it is considered as a failure to identify the stars, but in the category of silence (Fig. 6). If a mismatch of the catalog number occurs between any of the simulated and the identified stars, the frame is categorized as wrongly identified.

13) Four attributes of performance, namely, percentage of the frames that are successfully identified, percentage of the failure to identify in the categories of silence, and wrong identification, along with the average computational time per frame are recorded for each test.

14) Note that the timing is recorded on a personal computer based on an AMD-K6-2 Processor with a 475-MHz clock speed running the Linux (RedHat distribution 8.0) operating system. The star identification program is compiled using GNU-C compiler with optimization at level 2. The timing refers to the CPU time obtained by the difference between two successive calls of clock subroutine of the operating system recorded before the star identification and after the postidentification scanning.

The results of the tests are given in the next section.

Table 2 Statistics of spikes injected in star simulation

Brightness error σ_m	Spikes/frame		Frames with at least 4 stars in C
	Mean	Standard deviation	
0.0	0.35	0.58	1000
0.1	0.35	0.59	1000
0.2	0.39	0.62	1000
0.3	0.45	0.65	1000
0.4	0.57	0.75	1000
0.5	0.72	0.84	1000
0.6	0.87	0.92	1000
0.7	1.06	1.01	1000
0.8	1.31	1.13	1000
0.9	1.45	1.17	1000
1.0	1.70	1.30	999
1.5	2.55	1.47	994
2.0	3.46	1.59	968

Results

In Tables 3 and 4, the results of the LIS star identification tests of the Pyramid method and the performance of the HASPID-K and HASPID-M methods for the same tests are listed. Figures 8 and 9 compare the results of all the above algorithms for LIS case only.

Location Error

Table 3 and Fig. 8 give the results of star identification when the location noise σ_{pix} of the star tracker is varied from 0 to 2.0 pixels (1σ) while the brightness noise σ_m is held constant at 0.3 magnitude (1σ). In Fig. 8a, the successful identification percentage of the new method remains as 100% up to 2.0-pixel location noise, whereas the Pyramid method retains it only up to 0.6-pixel noise. The latter starts to drop in the identification percentage beyond that noise level. This results in the rise of the percentage of silence in Fig. 8b in the Pyramid case. The wrong identifications of stars are minimal in all of the methods, even in the presence of large location noise, as indicated by Fig. 8c. Both of the new methods are faster in execution compared to the Pyramid up to 0.8-pixel noise, as indicated in Fig. 8d.

Brightness Error

Table 4 and Fig. 9 indicate the performance of all of the star identification algorithms under a test when the brightness noise σ_m of the star tracker is varied from 0 to 2.0 magnitude (1σ) while the location noise σ_{pix} is held constant at 0.5 pixels (1σ). The successful

Table 3 Sensitivity of the star identification with location error σ_{pix} and a constant brightness error, $\sigma_m = 0.3$ magnitude

	Success[b]			Silence[b]			Wrong[b]			Time, ms		
σ_{pix}[a]	Pyramid method	HASPID-K method	HASPID-M method	Pyramid method	HASPID-K method	HASPID-M method	Pyramid method	HASPID-K method	HASPID-M method	Pyramid method	HASPID-K method	HASPID-M method
0.0[c]	100.0	100.0	100.0	0.0	0.0	0.0	0.0	0.0	0.0	14.4	0.4	6.4
0.1[c]	100.0	100.0	100.0	0.0	0.0	0.0	0.0	0.0	0.0	15.3	0.4	6.3
0.2[c]	100.0	100.0	100.0	0.0	0.0	0.0	0.0	0.0	0.0	18.0	0.4	6.4
0.3[c]	100.0	100.0	100.0	0.0	0.0	0.0	0.0	0.0	0.0	14.0	0.5	7.4
0.4[c]	100.0	100.0	100.0	0.0	0.0	0.0	0.0	0.0	0.0	13.7	0.5	8.0
0.5	100.0	100.0	100.0	0.0	0.0	0.0	0.0	0.0	0.0	13.9	0.5	8.5
0.6	100.0	100.0	100.0	0.0	0.0	0.0	0.0	0.0	0.0	36.5	0.6	8.3
0.7	93.1	100.0	100.0	6.9	0.0	0.0	0.0	0.0	0.0	34.6	0.6	8.5
0.8	57.2	100.0	100.0	42.7	0.0	0.0	0.1	0.0	0.0	13.1	0.7	8.6
0.9	19.9	100.0	100.0	80.1	0.0	0.0	0.0	0.0	0.0	4.6	0.8	8.4
1.0	4.7	100.0	100.0	95.3	0.0	0.0	0.0	0.0	0.0	1.2	0.9	8.7
1.5	0.0	100.0	100.0	100.0	0.0	0.0	0.0	0.0	0.0	0.3	1.3	8.7
2.0	0.0	100.0	100.0	100.0	0.0	0.0	0.0	0.0	0.0	0.3	1.8	9.1

[a]Location error σ_{pix} in pixels. [b]Percentage of frames. [c]Thresholds ϵ, t_{angl}, and t_{cone} correspond to $\sigma_{pix} = 0.5$ pixel.

Table 4 Sensitivity of star identification with brightness error σ_m and constant location error, $\sigma_{pix} = 0.5$ pixel

	Success[b]			Silence[b]			Wrong[b]			Time, ms		
σ_m[a]	Pyramid method	HASPID-K method	HASPID-M method	Pyramid method	HASPID-K method	HASPID-M method	Pyramid method	HASPID-K method	HASPID-M method	Pyramid method	HASPID-K method	HASPID-M method
0.0[c]	100.0	100.0	100.0	0.0	0.0	0.0	0.0	0.0	0.0	14.9	0.5	4.1
0.1[c]	100.0	100.0	100.0	0.0	0.0	0.0	0.0	0.0	0.0	15.6	0.4	3.0
0.2[c]	100.0	100.0	100.0	0.0	0.0	0.0	0.0	0.0	0.0	12.6	0.5	6.8
0.3	100.0	100.0	100.0	0.0	0.0	0.0	0.0	0.0	0.0	14.0	0.4	8.2
0.4	100.0	100.0	100.0	0.0	0.0	0.0	0.0	0.0	0.0	17.8	0.6	16.6
0.5	99.8	100.0	100.0	0.2	0.0	0.0	0.0	0.0	0.0	18.3	1.1	31.3
0.6	99.9	100.0	99.9	0.1	0.0	0.1	0.0	0.0	0.0	22.7	1.6	43.0
0.7	99.8	100.0	100.0	0.2	0.0	0.0	0.0	0.0	0.0	18.6	1.9	56.3
0.8	99.6	100.0	100.0	0.4	0.0	0.1	0.0	0.0	0.0	24.4	2.7	80.7
0.9	99.6	100.0	100.0	0.4	0.0	0.3	0.0	0.0	0.0	27.2	3.4	128.3
1.0	99.4	99.9	99.9	0.6	0.1	0.1	0.0	0.1	0.0	34.3	4.7	210.4
1.5	97.1	99.1	99.1	2.6	0.8	0.8	0.3	0.0	0.1	54.9	11.3	785.4
2.0	92.0	96.8	96.7	7.3	3.1	3.1	0.7	0.1	0.2	78.0	25.8	2198.9

[a]Brightness error σ_m in magnitude. [b]Percentage of frames. [c]Magnitude threshold corresponds to $\sigma_m = 0.3$ magnitude.

identification percentage is 100% for both new methods up to 0.9 magnitude noise, whereas it remains at 100% up to 0.4 magnitude noise for the Pyramid method with a slight fall in percentage that is noticeable thereafter for Pyramid, as seen in Fig. 9a. It remains above 96.7% even at 2.0 magnitude noise for the HASPID-K and HASPID-M methods, whereas for Pyramid it is significantly lower at 92% at the same brightness noise. The failure in the identification yields mainly silence from all of the algorithms, as shown in Fig. 9b. The wrong identifications for Pyramid method is at 0.7% at 2.0 magnitude noise, whereas it is below 0.2% for the new methods as seen in the Fig. 9c.

As shown in Fig. 9c, the new method HASPID-K is faster in execution compared to the Pyramid method at all brightness noise levels and spikes. The HASPID-M method shows faster execution times up to a noise level of 0.4 magnitude when compared to Pyramid. The new HASPID-M method shows an exponential increase in the execution time with 2199 compared to 78 ms for Pyramid for 2.0 magnitude noise as logged in Table 4.

Numerical Accuracy

Finally, to examine the numerical accuracy of the simulations and their results, a test case of 0.5-pixel location noise and 0.3 magnitude brightness noise (both 1σ) is repeated 20 times. Each simulation run is made with a different seed value for the random number generator (RNG). The results of this test are given in Table 5.

These results are analyzed in the next section.

Table 5 Star identification test results with constant location error $\sigma_{pix} = 0.5$ pixel and constant brightness error $\sigma_m = 0.3$ magnitude

	Success[a]		Silence[a]		Wrong[a]		Time, ms	
Method	Mean	3σ	Mean	3σ	Mean	3σ	Mean	3σ
Pyramid	99.97	0.13	0.02	0.12	0.01	0.07	15.59	4.52
HASPID-K	100.0	0.07	0.01	0.07	0.0	0.0	0.47	0.12
HASPID-M	100.0	0.07	0.01	0.07	0.0	0.0	9.4	2.8

[a]Percentage of frames.

Analysis

In the test for the sensitivity of star identification with the location error, both the new methods based on the DAV algorithm score better than the Pyramid technique in all four attributes of performance. Surprisingly, the new methods perform faster than the Pyramid method that relies on the K-vector database of star pair angular separation even in a LIS condition. Even though the HASPID-K method utilizes the K-vector database, it filters out many spurious matches based on star magnitude match. The order of picking the most likely stars for the pivots based on their brightness in the spiral search that also matches their angular separation provides the necessary speed for HASPID-M.

On the other hand, the consistency checks among the probable star pairs for each side of the star polygon consume a lot of time for the Pyramid algorithm. This method inherently looks for a unique catalog triad combination for each measured triad and spends considerable time waiting for its occurrence. This weakness is clearly apparent when the execution time of the Pyramid method peaks in Fig. 8d under a higher location noise between 0.6 and 0.7 pixel. Beyond the 0.8 pixel noise, the Pyramid method consumes less time because it decides early to keep silent on the problem based on the strength of its probability calculation. This approach has yielded

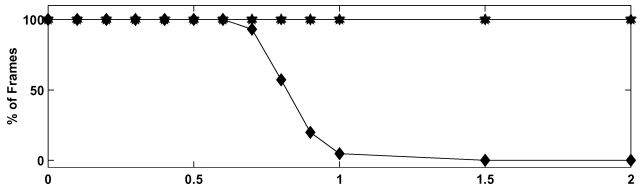

a) Successful star identification

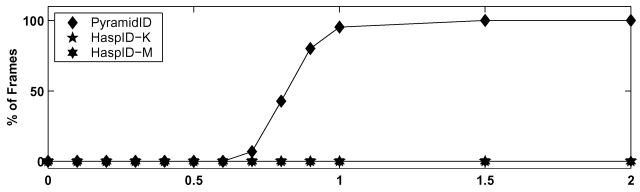

b) Silence in star identification

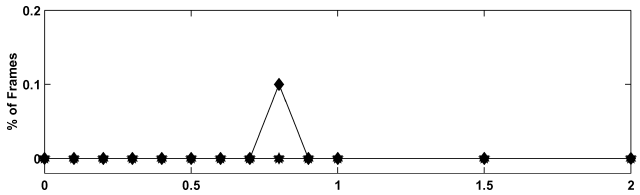

c) Wrong star identification

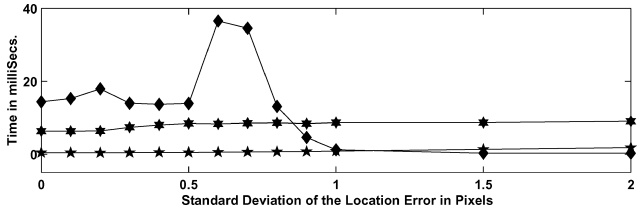

d) Computation time

Fig. 8 Sensitivity of identification with location error.

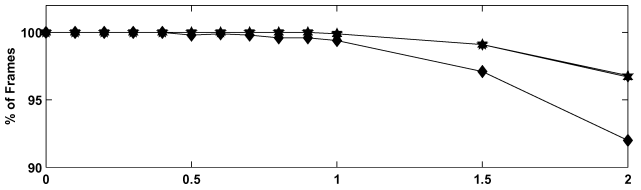

a) Successful star identification

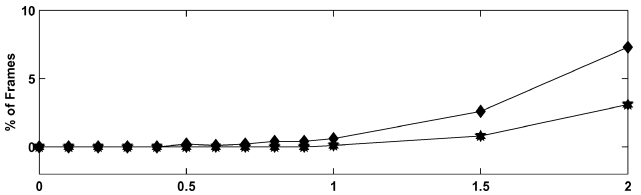

b) Silence in star identification

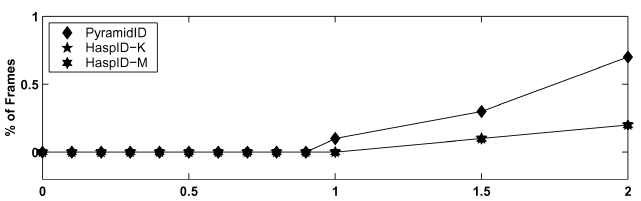

c) Wrong star identification

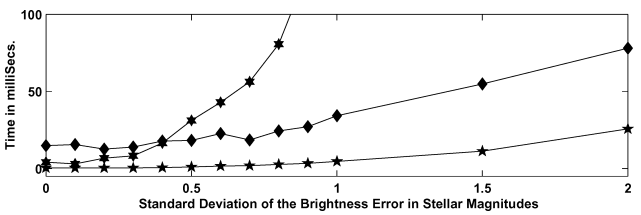

d) Computation time

Fig. 9 Sensitivity of identification with brightness error.

very few wrong identifications, but has resulted in silence when a large perturbation to star measurements is given. The new methods show good robustness in star identification, even in those noisy conditions because of the scientific utilization of the brightness information in addition to the angular separation of the stars.

In the second test for the sensitivity of star identification for the brightness error, the new HASPID-K and HASPID-M methods successfully identify 5% more frames than the Pyramid technique at 2.0 magnitude brightness noise (1σ). The drop in the identification percentage from the ideal (100%) is mainly due to the increased number of spikes present in the measurement. At 2.0 magnitude noise, only 6.5 out of 10 stars on an average are genuine stars and only 968 frames contain at least 4 stars of C as seen from the Table 2. Under this circumstance, the successful identification percentage returned by the new methods is probably the best that can be achieved. Even the wrong identification by the new methods is lower at 0.2% compared to 0.7% for Pyramid.

The new HASPID-K method has identified stars faster than Pyramid at all levels of brightness noise. HASPID-M method has shown an interesting trend. Although it is faster than Pyramid at lower level of brightness noise, it has shown exponential growth trend. This behavior of the new method is expected because the spiral search space expands exponentially with the brightness error from the Eq. (15). A penalty is paid for the on-the-fly search of the correct candidate star pair match by the new method. Because the adoptive thresholds are based on the brightness noise, it amounts to the search of the entire star catalog for the correct candidate pair for noise higher than 0.8 magnitude.

However, in-flight tests of the modern star trackers[9,10,18] result in better than 0.5 pixel and 0.25 magnitude random noise (1σ) and this can be reduced even further by time averaging, suggested in the spacecraft incremental-angle and angular velocity estimation method.[16] Under those practical noise levels, the new HASPID-M method, albeit without the support of angular separation database, can be used safely for star identification even in the LIS case. The new star identification methods based on the DAV algorithm exhibit better robustness compared to the Pyramid method even in the presence of a large perturbation to the star brightness measurements and spikes.

The timing measurements reported in Tables 3 and 4 show minor variations (although within the 3σ limits given in Table 5) for different Monte Carlo experiments. This difference is attributed to the functioning of simulation software under the multitasking operating system Linux. In addition, due to the selection of a different seed of RNG and variation in star sighting conditions for each experiment, there is a larger variation of time logged as seen from 3σ limits column in Table 5 for all three methods.

Note that the accuracy of the computed attitude matrix $\boldsymbol{D}_{I \to B}$ using the Triad method in the new proposed algorithms is only coarse because it is based only on two star observations. This may serve adequately to initialize a Kalman filter (see Ref. 16) that might be used later for precise attitude estimation. Alternatively, the star observations and their identified catalog stars may be subject to other attitude estimation programs such as FOAM,[8] QUEST,[7] ESOQ-2,[20] etc., for a finer accuracy because these methods use all of the available measurements in a least-square error minimization principle.

Conclusions

Two star pattern identification algorithms that can be used for a wide range of observation fields are developed from the classic DAV technique. In first method, the magnitude of the bright and dim stars is systematically used to eliminate the spurious matches in conjunction with an angular separation database. A novel spiral search that limits the exploration zone is used in the second method in lieu of

the separation database. Outline of the algorithms and flowcharts are given along with the rationale. The methods do not require a priori attitude, but can make use of any orientation knowledge of the spacecraft and its uncertainty. A hash table based on the direction and another index based on the brightness of the star catalog are used for speedy identification of the stars. The inertial attitude corresponding to the observed star pattern given by this method, though of coarse accuracy, may serve adequately to initialize an attitude determination Kalman filter.

In the numerical simulation tests conducted, the successful identification in LIS condition is close to 100% for reasonable perturbation levels (0.5-pixel location and 0.3 magnitude brightness noise, both 1σ) that are expected of modern star trackers. During the sensitivity tests, the algorithm has shown better robustness even at higher measurement noise when compared to another contemporary star identification algorithm, Pyramid. The execution time of the first method is at least 67% better than the Pyramid algorithm at all noise levels. However, the second method shows an interesting trend with a faster performance up to 0.4 magnitude (1σ) noise compared to Pyramid, although beyond that, it has an exponential increase in the identification process time.

Acknowledgments

We thank G. Madhavan Nair, chairman of the Indian Space Research Organization (ISRO) and K. N. Shankara, director of ISRO satellite center for their encouragement. Thanks are due to the editors and reviewers of the journal for their contribution in shaping this paper. Thanks are also due to the Linux, GNU, and Kdevelop community for providing their excellent software tools that have been used in this study extensively.

References

[1]Liebe, C. C., "Star Trackers for Attitude Determination," *IEEE Aerospace and Electronic Systems Magazine*, Vol. 10, No. 6, 1995, pp. 10–16.

[2]Gottlieb, D. M., and Wertz, J. R., *Spacecraft Attitude Determination and Control*, Kluwer Academic, Dordrecht, The Netherlands, 1978, reprinted 1991, pp. 26–28, 143–150.

[3]Van Bezooijen, R. W. H., "Autonomous Star Referenced Attitude Determination," *Guidance and Control*, Vol. 68, *Advances in Astronautical Sciences*, American Astronautical Society, San Diego, CA, 1989, pp. 31–52; also Paper AAS89-003, Feb. 1989.

[4]Baldini, D., Barni, M., Foggi, A., Benelli, G., and Mecocci, A., "A New Star-Constellation Matching Algorithm for Satellite Attitude Determination," *ESA Journal*, Vol. 17, No. 2, 1993, pp. 185–197.

[5]Padgett, C., and Delgado, K. K., "A Grid Algorithm for Autonomous Star Identification," *IEEE Transactions on Aerospace and Electronic Systems*, Vol. 33, No. 1, 1997, pp. 202–213.

[6]Blanton, J. N., "Star Identification for Sensors with Nonsimultaneous Acquisition Times," *Journal of the Astronautical Sciences*, Vol. 30, No. 3, 1982, pp. 277–285.

[7]Shuster, M. D., and Oh, S. D., "Three Axis Attitude Determination from Vector Observations," *Journal of Guidance, Control, and Dynamics*, Vol. 4, No. 1, 1981, pp. 70–77.

[8]Markley, F. L., "Attitude Determination Using Vector Observations: A Fast Optimal Matrix Algorithm," *Journal of the Astronautical Sciences*, Vol. 41, No. 2, 1993, pp. 261–280.

[9]Bank, T., "All Stellar Attitude Estimation Using a Ball CT-633 Star Tracker," *Guidance and Control*, *Advances in Astronautical Sciences*, American Astronautical Society, San Diego, CA, 1995, pp. 59–66; also Paper AAS95-004, Feb. 1995.

[10]Blarre, L., Thomas, S., Jacob, P., Foisneau, T., Vilaire, D., and Pochard, M., "Night Sky Tests and In-Flight Results of SED16 Autonomous Star Sensor," *Control and Guidance*, Vol. 113, *Advances in the Astronautical Sciences*, American Astronautical Society, San Diego, CA, 2003, pp. 389–398; also Paper AAS-03-043, Feb. 2003.

[11]Strunz, H. C., Baker, T., and Ethridge, D., "Estimation of Stellar Instrument Magnitudes," *Space Guidance, Control, and Tracking*, Vol. 1949, Proceedings of SPIE, International Society for Optical Engineering, Washington, DC, 1993, pp. 228–235.

[12]Mortari, D., Junkins, J. L., and Samaan, M. A., "Lost-In-Space Pyramid Algorithm for Robust Star Pattern Recognition," *Control and Guidance*, Vol. 107, *Advances in the Astronautical Sciences*, American Astronautical Society, San Diego, CA, 2001, pp. 49–68; also Paper AAS-01-004, Feb. 2001.

[13]Mortari, D., "Search-Less Algorithm for Star Pattern Recognition," *Journal of the Astronautical Sciences*, Vol. 45, No. 2, 1997, pp. 179–194; also American Astronautical Society Paper AAS-96-158, Feb. 1996.

[14]Hall, R. W., "Efficient Spiral Search in Bounded Spaces," *IEEE Transactions on Pattern Analysis and Machine Intelligence*, Vol. PAMI-4, No. 2, 1982, pp. 208–215.

[15]Rao, G. N., Bhat, M. S., and Alex, T. K., "Fast Access Method for Onboard Star Catalog," *Journal of Guidance, Control, and Dynamics*, Vol. 28, No. 5, 2005, pp. 1032–1037.

[16]Rao, G. N., Alex, T. K., and Bhat, M. S., "Incremental-Angle and Angular Velocity Estimation Using a Star Sensor," *Journal of Guidance, Control, and Dynamics*, Vol. 25, No. 3, 2002, pp. 433–441.

[17]Padgett, C., Kreutz-Delgado, K., and Udomkesmalee, S., "Evaluation of Star Identification Techniques," *Journal of Guidance, Control, and Dynamics*, Vol. 20, No. 2, 1997, pp. 259–267.

[18]Vandana Singh, Pullaiah, D., Rao, J. S., Shashikala, T. H., Rao, G. N., Jain, Y. K., and Alex, T. K., "Generation and Validation of On-Board Star Catalog for Resourcesat-I Star Tracker," *Astrodynamics Specialist Conference*, Vol. 3, AIAA, Reston, VA, 2004, pp. 1530–1535.

[19]Kreyszig, E., *Advanced Engineering Mathematics*, 5th ed., Wiley Eastern, New Delhi, India, 1983, pp. 927–931.

[20]Mortari, D., "Second Estimator of the Optimal Quaternion," *Journal of Guidance, Control, and Dynamics*, Vol. 23, No. 5, 2000, pp. 885–887.